Host–Guest Systems

Deutsche Ausgabe: DOI: 10.1002/ange.201510637
Internationale Ausgabe: DOI: 10.1002/anie.201510637

Guest-Induced Breathing Effect in a Flexible Molecular Crystal

Yujie Sheng, Qibin Chen, Junyao Yao, Yunxiang Lu, Honglai Liu,* and Sheng Dai**

Abstract: *By introducing a flexible component into a molecular building block, we present an unprecedented alkyl-decorated flexible crystalline material with a breathing behavior. Its selective adsorption is derived from the breathing effect induced by a guest triggered alkyl transformation. This feature allows the crystal to take up 2.5 mmol g^{-1} of chloroform with high adsorption selectivity ($CHCl_3$/EA > 2000 for example), implying a potential application in sorption separation and chemical sensors.*

The uptake and encapsulation of guest species by microporous materials has great potential in a wide range of applications, such as selective molecular separations, chemical sensing, heterogeneous catalysis, and gas storage.[1] Over the past few years porous molecular crystals (PMCs) have evolved as a promising alternative to traditional adsorbents, such as zeolites, activated carbon, metal–organic frameworks (MOFs), covalent organic frameworks, or network polymers, because of their distinguishing features.[2] Generally, PMCs should be fabricated by removal of solvent molecules from their inclusion crystals.[3] However, a major challenge is that PMCs do not commonly retain their incipient porosity upon guest removal, but rather collapse to form a dense phase. Thus, a more general design strategy would incorporate molecular rigidity into building blocks to prevent precursors from close-packing during evacuation.[4] In other words, molecular flexibility has to be avoided. In contrast, to control the pore size and achieve switchable processes in MOFs, flexible components (namely metal ions and organic linkers) are usually employed.[5] For example, a reversible open-dense framework transformation was successfully facilitated by distorting nodes and bending struts.[6] Moreover, MOFs can enable enhanced selective guest sorption in response to external stimuli by a gate-opening effect resulting from the structural transformation of a flexible architecture.[7] Inspired by PMC and MOF design concepts, we propose construction of a new bimodal PMC containing rigid and flexible moieties in one assembly unit, where the former are responsible for retaining the integral scaffold, while the latter are responsible for a structural transformation response to external stimuli.

Recently, we found that a Gemini surfactant composed of two alkyl chains, a typical flexible group, and a rigid biphenyl spacer, formed a crystal in which water was included.[8] Unfortunately, stability of the crystal was lost upon guest removal. Nevertheless, because such Gemini molecules possess both rigid and flexible groups, we hypothesized that construction of a novel PMC with an external stimulus-responsive behavior arising from the structural transformation of alkyl chains was reasonable.

The primary objective of this work was to test this hypothesis by changing the spacer and the crystallizing method, with a view to enhancing the crystal stability during guest removal. With this purpose in mind, we synthesized a new Gemini surfactant, *N*,*N*′-((diazene-1,2-diylbis(4,1-phenylene))bis(methylene))bis(*N*,*N*-dimethyl-dodecan-1-ammonium) bromide (Scheme 1), by introducing an azobenzene spacer into the structure (see Supporting Information). A flexible PMC was grown by liquid phase diffusion of tetrachloroethane into an ethyl acetate solution of the Gemini surfactant, producing PMC-1. Intriguingly, PMC-1 only responds to chloroform vapor, exhibiting a reversible adsorption–desorption process after exposure to chloroform vapor and nitrogen atmosphere, thus indicating a better selectivity for chloroform compared to other organic vapors. This preferential sorption property probably stems from the formation of transient pores, which originate from the bending of terminal chains in PMC-1 as they accommodate guest molecules. Simultaneously, the structural transformation of flexible moieties and adsorption–desorption of chloroform lead to a reversible expansion/shrinkage of the PMC-1 unit cell.

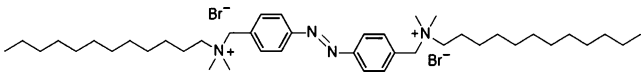

Scheme 1. Molecular structure of a Gemini molecule employed as a PMC (porous molecular crystal) building block.

Initially, we examined the N_2 adsorption–desorption isotherm of PMC-1. The isotherm plot showed that PMC-1 takes up extremely low volumes of N_2 gas at low relative-pressures at 77 K (Supporting Information, black scatter in Figure S1). Thus, PMC-1 was deemed to be non-porous. A low 8.1 m^2 g^{-1} Brunauer–Emmett–Teller surface area may be attributed to the solid surface and piled pores of crystal particles. Despite this, we investigated the properties of the material at 298 K with the aim of understanding whether thermal stimuli could "activate" the transition of alkyl chains,

[*] Y. Sheng, Prof. Q. Chen, J. Yao, Dr. Y. Lu, Prof. H. Liu
State Key Laboratory of Chemical Engineering, Department of Chemistry, East China University of Science and Technology
Shanghai, 200237 (P.R. China)
E-mail: qibinchen@ecust.edu.cn
hlliu@ecust.edu.cn
Prof. S. Dai
Chemical Sciences Division, Oak Ridge National Laboratory
Oak Ridge, TN 37831 (USA)
and
Department of Chemistry, University of Tennessee
Knoxville, TN 37996-1600 (USA)
E-mail: dais@ornl.gov

Supporting information for this article is available on the WWW under http://dx.doi.org/10.1002/anie.201510637.

and in so doing generate void spaces. Unfortunately, this hypothesis was not substantiated (Supporting Information, red scatter in Figure S1).

Surprisingly, PMC-1 showed a significant uptake of $CHCl_3$ when exposed to chloroform vapor in the low relative-pressure region at 298 K (Figure 1 a). The isotherm curve of $CHCl_3$ revealed a steep rise in the range of p/p_0 from about 0.02–0.06. A plateau after saturation suggested that PMC-1 is porous to $CHCl_3$. Desorption of $CHCl_3$ only starts at $p/p_0 <$ 0.055, resulting in a hysteresis loop with a width of 0.66 kPa. Hysteresis can be attributed to significant adsorbent–adsorbate interactions arising from hydrogen-bonding or dipole–dipole contacts.[9] In contrast, it is surprising that for other volatile organic compounds (VOCs) PMC-1 reveals a slight linear or level uptake, indicating that this material appears to be essentially non-porous to such VOCs. These results are consistent with the N_2 adsorption–desorption isotherms. Here, a molecular sieving effect by PMC-1 should be ruled out because the molecules employed are of a size less than that of $CHCl_3$, and have a low CH_2Cl_2, CH_3OH, and C_2H_5OH uptake, and a negligible N_2 uptake. It is worth noting that PMC-1 crystal particles agglomerated above the relative-pressure mid-range when a routine gas-adsorption measurement method was used to determine adsorption–desorption characteristics of the four VOCs ($CHCl_3$, CH_2Cl_2, CH_3OH, and C_2H_5OH). Therefore, we focused on the sorption properties in the low relative-pressure region in case of the occurrence of capillary condensation. These results suggest that PMC-1 responds exclusively to $CHCl_3$ vapor as a result of structural transition. Furthermore, 10 repeated sorption cycles clearly demonstrate that PMC-1 can adsorb/desorb $CHCl_3$ with good reproducibility, indicating that structural transformations are reversible (Figure 1 b).

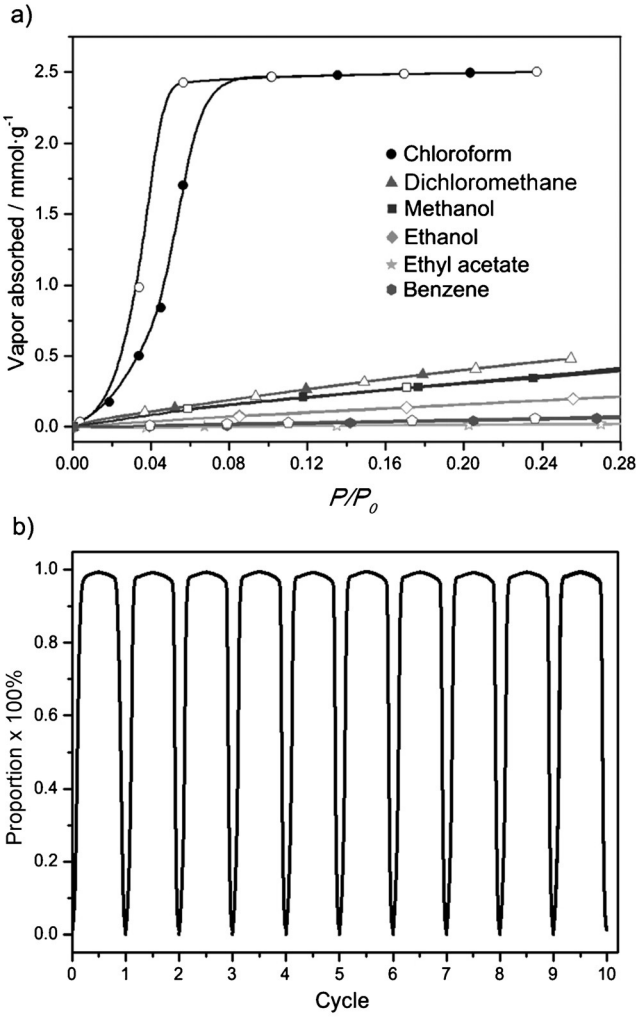

Figure 1. The adsorption–desorption isotherms of PMC-1 for various VOCs at 298 K. a) Adsorption (closed symbols)–desorption (open symbols) isotherms for VOCs. b) Adsorption–desorption cycles for $CHCl_3$. P_0 for VOCs: chloroform 26.54 kPa, dichloromethane 53.33 kPa, methanol 8.205 kPa, ethanol 16.98 kPa, ethyl acetate 13.33 kPa, benzene 12.69 kPa.

In Figure 1 a, $CHCl_3$ uptake is close to 2.5 mmol g^{-1}, comparable to that of other porous networks.[10] PMC-1 demonstrates slight adsorption of the other VOCs, consequently enabling a high selective adsorption of $CHCl_3$ over the other VOCs. For example, the ratio of $CHCl_3$/EA selectivity exceeds 2000 (Supporting Information, Table S1). Even the low $CHCl_3/CH_2Cl_2$ selectivity (ca. 14) determined by our work is an order of magnitude higher than that described in previous reports.[11] For practical applications, adsorption–desorption rates were evaluated using mass variation by alternatively exposing PMC-1 to a N_2 stream saturated with $CHCl_3$ vapor and a dry N_2 stream. The adsorption process took only six minutes to reach saturation in a $CHCl_3/N_2$ mixture, while the desorption process took one hour under N_2 purging (Supporting Information, Figure S2). Moreover, agglomeration of PMC-1 particles did not take place in the $CHCl_3/N_2$ mixture, unlike the situation described above using routine methods. Although we did not understand the reason for this behavior, avoidance of the agglomeration phenomenon renders PMC-1 a suitable material for practical applications.

Remarkably, the inclusion single crystal PMC-2 was obtained after exposure of PMC-1 to a $CHCl_3/N_2$ mixture atmosphere for about an hour at room temperature.[12] The unique $CHCl_3$ induced response of PMC-1 prompted us to elucidate structural transitions using single-crystal structure analysis. Both PMC-1 and PMC-2 were characterized by thermogravimetric analysis (TGA), X-ray diffraction (XRD), and single-crystal X-ray diffraction (SC-XRD). TGA results indicate that PMC-1 is a completely desolvated crystal, while PMC-2 is solvated with two $CHCl_3$ molecules per host molecule (Supporting Information, Figure S3). According to the XRD patterns, PMC-2 is able to recover to PMC-1 by means of a thermal treatment ($< 75\,^{\circ}C$) or N_2 sweeping (Supporting Information, Figure S4). Moreover, a reversible transition is confirmed by the single-crystal diffraction results from desolvated PMC-2 (Supporting Information, Figure S5 and Table S3).

Single-crystal XRD patterns indicate that both PMC-1 and PMC-2 are in the same Pbcn space group (crystal details are summarized in the Supporting Information, Table S2). Structural analysis of PMC-1 in Figure 2 a revealed a number of key features: 1) all of the Gemini molecules adopt a zigzag conformation and their alkyl chains align adjacent to benzene

rings to form a 1D column along the *c* axis as a result of C–H···π interactions (a 4.62 Å distance from the antepenultimate carbon atom of terminal alkyl chains to the center of the adjacent benzene ring; Supporting Information, Figure S6);[13] 2) two such columns stack face to face to form a pair of columns connected by electrostatic attractions between quaternary ammonium head groups and counterions (Supporting Information, Figure S7), π–π stacking and C–H···π interactions (a 3.88 Å distance from the middle of the alkyl chain to the center of the benzene ring of the neighboring layer; Supporting Information, Figure S8); and 3) column pairs align in a staggered lattice because of electrostatic attractions in the *aob* plane, thereby forming the PMC-1 host scaffold. The space-filling model of the crystal is densely packed without substantial voids (Supporting Information, Figure S9), rendering the PMC an impractical host for atoms or molecules. The framework cannot even accommodate H^+ ions. Unremarkable adsorption of VOC vapors are a likely consequence of the space restrictions in the crystal, except in the case of $CHCl_3$.

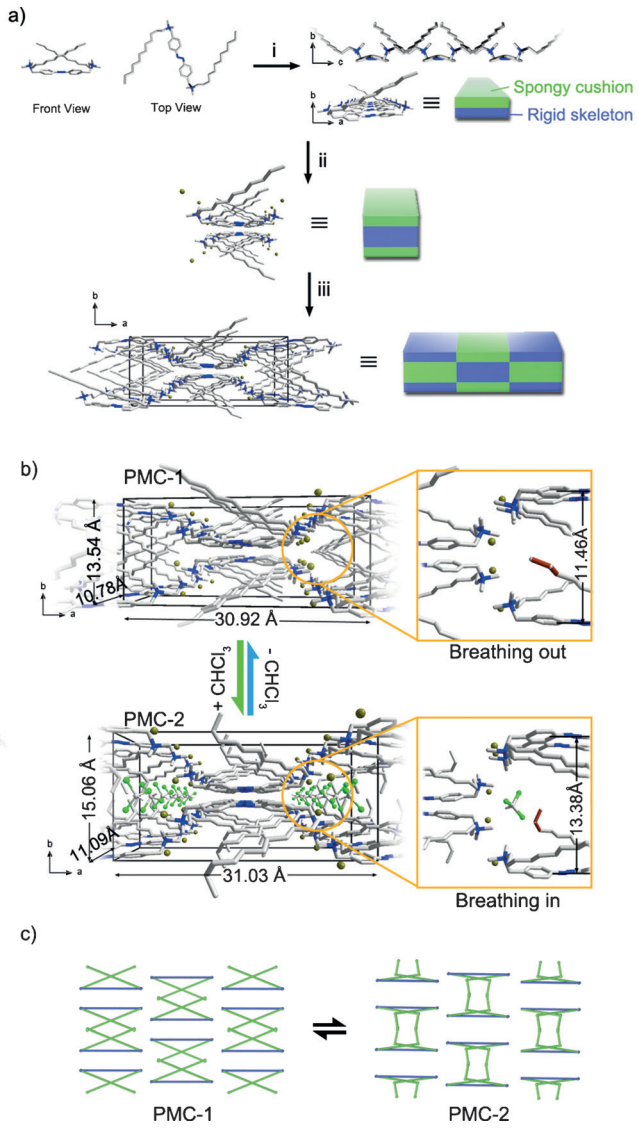

Figure 2. Stacking process of PMC-1 and structural variation before and after guest encapsulation. a) Representation of the PMC-1 assembly process. b) Unit cell expansion/shrinkage and alkyl transformation during adsorption–desorption processes. C gray, N blue, Cl green, Br olive. Hydrogen atoms are omitted for clarity. c) A representation of transitions in framework topology between PMC-1 and PMC-2.

In sharp contrast, PMC-2 is formed after exposure to chloroform with a unit cell volume increase of about 15%, from 4513 (PMC-1) to 5185 (PMC-2) $Å^3$. The size of the unit cell in *b* and *c* directions increases by 11.22% and 2.88%, respectively, with near retention of length along the *a* axis (Figure 2b). Overall, the assembly motif of PMC-2 is similar to that of PMC-1. However, closer inspection of substructures shows several points of difference. Firstly, the localized amplified images reveal that the terminal alkyl chain (brown) transforms from an all-*trans* conformation to partially *gauche* upon guest adsorption. Secondly, the inter-plane distance between the two neighboring azo planes, which belong to two adjacent column pairs, increased from 11.46 Å to 13.38 Å. Thirdly, alkyl chains are pushed towards the rigid spacer, compressing intermolecular C–H···π interactions from 4.62 Å to 3.71 Å (Supporting Information, Figure S6). These transformations in structure lead to an expanded scaffold and generate many larger transient pores for accommodation of $CHCl_3$.[14] Consequently, the adsorption–desorption of guests endows PMC-1 with a "breathing" characteristic, closely related to the expansion–shrinkage of its scaffold (Figure 2c).

Breathing effects can be attributed to the unique molecular structure of the Gemini molecule and its packing motif. As expected, azobenzene spacers facilitate fabrication of a rigid scaffold which is immovable in both PMC-1 and PMC-2, while alkyl chains are the origin of structural transformation. When Gemini molecules assemble along one direction, rigid spacers adopt the same orientation and alkyl chains orient to one side. Thus, the resulting molecular column can be regarded as a skeleton covered with a spongy cushion on one side (represented by blue and green boxes in Figure 2a). Columns of this type stack in pairs to form a column pair because of electrostatic, π–π stacking and C–H···π interactions, thereby formulating the building unit ("brick") of each PMC. The skeleton moieties of these bricks are connected through electrostatic interactions (Supporting Information, Figure S10) and form a stable scaffold in which spongy cushions (flexible alkyl chains) are filled. During the adsorption process, guest molecules ingress into the spongy moieties, leading to a structural transformation. Adjacent bricks are compressed and transient pores are formed to accommodate guest molecules (Supporting Information, Figure S11). Upon guest evacuation, the spongy cushion recovers to its original state and the PMC converts into a dense staggered arrangement, akin to a brick wall.

When guest molecules squeeze into voids, fully extended alkyl chains are compelled to adopt a *gauche* conformation because of their flexibility. As a result the scaffold expands simultaneously. This thermodynamically unfavorable process requires additional energy, which can only stem from affinity between the guest molecule and the scaffold. In PMC-2, host–guest affinity mainly comes from hydrogen bonding interactions, which are summarized in Table S4 (Supporting

Information). The interaction between scaffold and $CHCl_3$ has a large binding affinity energy of $-14.8\ kcal\,mol^{-1}$ according to DFT calculations[15] and non-covalent interaction (NCI) analysis[16] (Supporting Information, Figure S12), which facilitates the structural transition of alkyl chains and volume expansion of the framework. For comparison, the binding energy affinity of other VOC molecules for $CHCl_3$ was also calculated (Supporting Information, Figure S13). Calculations indicate that none of the other VOCs possess an affinity for $CHCl_3$ as great as that shown by PMC-1. Logically, molecules larger in size than $CHCl_3$ require a higher additional energy to induce a more expansive transition in the PMC-1 structure. The affinity between bigger molecules and the scaffold was not determined in this case, but it is anticipated that variations in binding affinity of different host–guest complexes will signal propensities for guest sorption.

In summary, we have confirmed that flexible components contribute to enhance the selectivity of porous molecular crystals. More importantly, we have described the first example of an alkyl decorated PMC for specific adsorption of VOCs. The fast adsorption rate and low-pressure saturation of PMC-1 lends the material to gas sensor applications for specific detection of chloroform. Our findings indicate that introduction of flexible components may facilitate the design of new functional PMCs.

Supporting information for this article may be accessed using the link at the end of the document. CCDC 1437194 and 1437195 contain the supplementary crystallographic data for this paper. Data can be obtained free of charge from The Cambridge Crystallographic Data Centre.

Acknowledgements

Y.J.S., Q.B.C., J.Y.Y., Y.X.L., and H.L.L. thank the National Natural Science Foundation of China (No.21273074, 91334203, 21576079), the 111 Project of China (No.B08021) and the Fundamental Research Funds for the Central Universities of China. SD was sponsored by the Division of Chemical Sciences, Geosciences, and Biosciences, Office of Basic Energy Sciences, U.S. Department of Energy.

Keywords: chloroform · host–guest systems · porous molecular crystals · preferential adsorption · self-assembly

How to cite: *Angew. Chem. Int. Ed.* **2016**, *55*, 3378–3381
Angew. Chem. **2016**, *128*, 3439–3442

[1] a) S. Horike, S. Shimomura, S. Kitagawa, *Nat. Chem.* **2009**, *1*, 695–704; b) L. Chen, P. S. Reiss, S. Y. Chong, D. Holden, K. E. Jelfs, T. Hasell, M. A. Little, A. Kewley, M. E. Briggs, A. Stephenson, K. M. Thomas, J. A. Armstrong, J. Bell, J. Busto, R. Noel, J. Liu, D. M. Strachan, P. K. Thallapally, A. I. Cooper, *Nat. Mater.* **2014**, *13*, 954–960; c) M. Zhao, S. Ou, C.-D. Wu, *Acc. Chem. Res.* **2014**, *47*, 1199–1207; d) R. E. Morris, P. S. Wheatley, *Angew. Chem. Int. Ed.* **2008**, *47*, 4966–4981; *Angew. Chem.* **2008**, *120*, 5044–5047.

[2] a) J. R. Holst, A. Trewin, A. I. Cooper, *Nat. Chem.* **2010**, *2*, 915–920; b) P. Li, Y. He, Y. Zhao, L. Weng, H. Wang, R. Krishna, H. Wu, W. Zhou, M. O'Keeffe, Y. Han, B. Chen, *Angew. Chem. Int. Ed.* **2015**, *54*, 574–577; *Angew. Chem.* **2015**, *127*, 584–587; c) P. Li, Y. He, J. Guang, L. Weng, J. C.-G. Zhao, S. Xiang, B. Chen, *J. Am. Chem. Soc.* **2014**, *136*, 547–549; d) J. Lü, C. Perez-Krap, M. Suyetin, N. H. Alsmail, Y. Yan, S. Yang, W. Lewis, E. Bichoutskaia, C. C. Tang, A. J. Blake, R. Cao, M. Schröder, *J. Am. Chem. Soc.* **2014**, *136*, 12828–12831.

[3] a) N. B. McKeown, *J. Mater. Chem.* **2010**, *20*, 10588–10597; b) O. Buyukcakir, Y. Seo, A. Coskun, *Chem. Mater.* **2015**, *27*, 4149–4155.

[4] M. Mastalerz, *Chem. Eur. J.* **2012**, *18*, 10082–10091.

[5] S.-i. Noro, D. Tanaka, H. Sakamoto, S. Shimomura, S. Kitagawa, S. Takeda, K. Uemura, H. Kita, T. Akutagawa, T. Nakamura, *Chem. Mater.* **2009**, *21*, 3346–3355.

[6] B. Chen, C. Liang, J. Yang, D. S. Contreras, Y. L. Clancy, E. B. Lobkovsky, O. M. Yaghi, S. Dai, *Angew. Chem. Int. Ed.* **2006**, *45*, 1390–1393; *Angew. Chem.* **2006**, *118*, 1418–1421.

[7] a) I. M. Hauptvogel, R. Biedermann, N. Klein, I. Senkovska, A. Cadiau, D. Wallacher, R. Feyerherm, S. Kaskel, *Inorg. Chem.* **2011**, *50*, 8367–8374; b) N. Nijem, H. Wu, P. Canepa, A. Marti, K. J. Balkus, T. Thonhauser, J. Li, Y. J. Chabal, *J. Am. Chem. Soc.* **2012**, *134*, 15201–15204; c) C. Wang, L. Li, J. G. Bell, X. Lv, S. Tang, X. Zhao, K. M. Thomas, *Chem. Mater.* **2015**, *27*, 1502–1516.

[8] a) Y. Sheng, J. Yao, Q. Chen, H. Liu, *CrystEngComm* **2015**, *17*, 1439–1447; b) Q. Chen, J. Yao, X. Hu, J. Shen, Y. Sheng, H. Liu, *J. Appl. Crystallogr.* **2015**, *48*, 728–735.

[9] H. J. Choi, M. Dincă, J. R. Long, *J. Am. Chem. Soc.* **2008**, *130*, 7848–7850.

[10] a) Y.-C. Chiang, P.-C. Chiang, C.-P. Huang, *Carbon* **2001**, *39*, 523–534; b) E. Ahmed, J. Khanderi, D. H. Anjum, A. Rothenberger, *Chem. Mater.* **2014**, *26*, 6454–6460; c) S. Van der Perre, T. Van Assche, B. Bozbiyik, J. Lannoeye, D. E. De Vos, G. V. Baron, J. F. M. Denayer, *Langmuir* **2014**, *30*, 8416–8424; d) H. Yamagiwa, S. Sato, T. Fukawa, T. Ikehara, R. Maeda, T. Mihara, M. Kimura, *Sci. Rep.* **2014**, *4*, 6247; e) K. Yang, Q. Sun, F. Xue, D. Lin, *J. Hazard. Mater.* **2011**, *195*, 124–131.

[11] a) M. Eddaoudi, H. Li, O. M. Yaghi, *J. Am. Chem. Soc.* **2000**, *122*, 1391–1397; b) F. Yang, Q.-K. Liu, J.-P. Ma, Y.-A. Li, K.-X. Wang, Y.-B. Dong, *CrystEngComm* **2015**, *17*, 4102–4109.

[12] It should be noted that PMC-2 shows localized uncertainty at the tip of the alkyl chains. This is because the transformation of flexible alkyl chain may undergo multiple metastable states with tiny difference. This situation also occured when we soaked PMC-1 in a saturated chloroform solution. Localized disorder does not affect our conlusions because we discuss only one position throughout the manuscript.

[13] M. J. Plevin, D. L. Bryce, J. Boisbouvier, *Nat. Chem.* **2010**, *2*, 466–471.

[14] a) S. A. Herbert, A. Janiak, P. K. Thallapally, J. L. Atwood, L. J. Barbour, *Chem. Commun.* **2014**, *50*, 15509–15512; b) L. J. Barbour, *Chem. Commun.* **2006**, 1163–1168; c) A. Kondo, N. Kojima, H. Kajiro, H. Noguchi, Y. Hattori, F. Okino, K. Maeda, T. Ohba, K. Kaneko, H. Kanoh, *J. Phys. Chem. C* **2012**, *116*, 4157–4162.

[15] Y. Liu, J. Zhao, F. Li, Z. Chen, *J. Comput. Chem.* **2013**, *34*, 121–131.

[16] E. R. Johnson, S. Keinan, P. Mori-Sánchez, J. Contreras-García, A. J. Cohen, W. Yang, *J. Am. Chem. Soc.* **2010**, *132*, 6498–6506.

Received: November 16, 2015
Revised: December 23, 2015
Published online: February 2, 2016

